

ARCHAOMETRIC STUDY AND CONSERVATION OF A GODDESS BASTET STATUE FROM THE LATE PERIOD OF ANCIENT EGYPT

Medhat ABDALLAH^{1*}, Mohamed MOUSTAFA², Ezzat M. MORSI¹, Gehan R. ALI¹

¹ Administration of Storerooms Conservation, Saqqara, Giza, Egypt

² Wood Laboratory, Conservation Center, The Grand Egyptian Museum, Giza, Egypt

Abstract

The wooden statue of the goddess Bastet, dates back to the Late period of ancient Egypt (664-332 BC), is the subject of this study. This archaeometric study aims to use investigation techniques including technical photography (TP), optical microscopy (OM), Energy Dispersive X-Ray Analysis (ESEM-EDX) and Fourier transformed infrared (FT-IR) spectroscopy to identify the components of the statue and to understand its deterioration aspects. The results revealed using six wood species including Lebanese Cedar, sycamore fig and Tamarisk for the body of the statue and its pedestal; while the dowels are made of Christ's thorn, Nile tamarisk and common box. Stratigraphy structure shows several and rare techniques of statuary-making. investigation techniques indicate that pigments used in the statue identified as calcium carbonate (chalk) for white, Egyptian blue for blue, hematite for red, the gilded layer is composed of a mixture of gold and silver. For the organic materials, we could recognize beeswax as a coating material and a plant gum as binder for red, yellow, while a proteinaceous-based binding medium is used for the Egyptian blue. To restore the statue, conservation procedures were used with great precision, including securing the vulnerable layer, cleaning, reattaching, and reassembly of the fragmented sections, as well as fixing fractures and separations. Finally, the conservation treatments were exceedingly efficient in restoring the statue's solidity and strength, allowing it to be shown or stored.

Keywords: Bastet; FTIR; EDX; Beeswax; Technical photography; Wood identification; Late period

Introduction

In ancient Egypt, religion had a significant part in daily life, the ancient Egyptian artisans made the statues to honor the deities; The variety of materials and techniques utilized in these sculptures demonstrates expert craftsmanship and a refined sense of beauty, many authors pay much interest to identify the components and techniques used in ancient Egyptian statuary-making; however, these statues need more scientifically investigations.

The *Bastet* statue under study (Fig. 1), dates back to the late period (664-332 BC), shows the diversity of materials and unusual techniques used in statuary-working in ancient Egypt and their reflection on manufacturing materials selection and deterioration aspects.

The purpose of this paper is to use a combination of scientific and investigation measurements to understand the techniques and materials employed in making the studied statue and characterize the role of conservation and developing the conservation procedure of loss compensation depending on ancient Egyptian techniques. The authors used optical microscopy and technical photography, as well as Energy Dispersive X-Ray Analysis and Fourier transform infrared spectroscopy, to map and identify the pigments and organic binding

* Corresponding author: medhat.a.abdelhamid@gmail.com

media used in the statue, and to gain a better understanding of the painting techniques and the object's condition.



Fig. 1. General view of the goddess *Bastet* statue before conservation: (a) the body of the statue. (b) The pedestal. (c) Inside the statue

Furthermore, we were particularly interested in wood species identification.

Description of the statue

The *Bastet* statue (Registration No.20199) was discovered in the necropolis of Saqqara in 2019 by the Egyptian mission headed by the general secretary of the supreme council of antiquities (SCA). The statue depicted the goddess *Bastet*, as a cat made of pieces of wood and textile coated with a thin layer of white plaster, the face is gilded; her eyes are inlaid and blue scarab inlaid in the head. The statue is hollow, a small mummy inside the statue, maybe a mummified cat. The statue was fixed on a richly decorated pedestal made of small pieces of wood collected together by wooden nails (Dowels) which coated with two white preparatory layers separated by black pigment, while the surface is decorated with polychrome scenes. Dimensions: H.67.5×W.27.5×D.56cm (including pedestal)

Materials and Methods

Visual assessment

Visual inspection was used to evaluate the features of degradation observed on the statue, with the help of the team's critical eye. Because the reasons and mechanisms of degradation may be easily identified, this strategy is particularly successful. The conservator's critical eye can also decide the most effective ways of study that should be used to evaluate the state of the statue being investigated.

Optical microscopy (OM)

Optical microscopy (OM), model XSZ-107BN, equipped with Amscop MD500 camera and software Amscop 3.7, was used to identify the wood species and textile threads detected on the statue under study (OM) model XSZ-107BN, equipped with Amscop MD500 camera and software Amscop 3.7. Wood samples were sliced into three anatomical directions: transverse section (TS), longitudinal radial section (LRS), and longitudinal tangential section (LTS) at 30–50µ, and then displayed on glass slides [1, 2].

To identify the textile's fibers; provided samples of fibers were soaked in glycerol then mounted on the slide glass. Wood samples and fibers were viewed under the microscope in transmitted light [3].

Digital USB microscopy

For identification of insects found inside the hollow pedestal; insects were carefully isolated and mounted on glass slides to be studied under reflected light by using USB Dino-lite digital microscope. USB digital microscope was used also for photographing and studying the characteristics of insect attacks and textile weaving quality.

Through comparison with descriptions accessible in textbooks, atlases, and websites, the taxon of wood species, insects, and kind of fibers may be identified.

Technical photography (TP)

A series of photographs obtained using a customized digital camera sensitive to the spectral region of around 360-1000 nm is referred to as technical photography (TP). A variety of illumination sources and filters are utilized to capture a variety of technical photographs, each of which provides unique information about the item under investigation. Technical photography (TP) is a non-invasive method of identifying and determining the spatial distribution of painting ingredients in a piece of art [4, 5], for example, ultraviolet-induced luminescence (UVL) is a standard technique for revealing the location of luminous compounds, such as current conservation products and a variety of old organic materials utilized in antiquity [6-9]. In museums, infrared reflectance (IRR) photography is most commonly employed to detect any preliminary sketches or carbon-based paints [10, 11], Infrared reflectance (IRR) is highly opaque to carbon, making this approach effective for mapping the location of carbon-based pigments [12].

Technical pictures were collected using Dino lite digital microscopy in this work, including visible light (VIS), ultraviolet-induced luminescence (UVL), visible-induced infrared luminescence (VIL), and infrared reflected (IRR) [6].

Egyptian blue has the ability to absorb visible light and reemit infrared (IR) light in the 800-1000 μm range, with a peak at c.910 nm (visible-induced luminescence). Because the pigment's IR emission is so powerful (Cuprorivaite is the strongest IR emitter currently known at a molecular level), the luminescence may be easily photographed in a darkened setting using a customized digital camera with some IR sensitivity. In order to acquire visible-induced infrared luminescence (VIL) images, the authors in this study have used Dino-lie microscope fitted with UV/Visible blocking filter (IR 87C filter) [13, 14].

Canon EOS 8xi is used for photography documentation of conservation procedures; To produce a camera profile for Adobe Camera Raw, the camera was calibrated with the X-rite Color Checker Passport and its included software. The photographs were captured in RAW format and subsequently color-corrected and white-balanced using the camera profile [6, 15].

Raking light is a method that illuminates the studied object from only one side, at an oblique angle to its surface. The surface roughness of a painting is revealed by raking light. Raised paint surfaces that face the light are lighted, whilst those that face away from the light cast shadows. The improved look of paint texture may be easily observed, photographed, or digitally recorded [16].

Energy Dispersive X-Ray Analysis (ESEM-EDX)

The Philips XL30 ESEM was used in conjunction with energy dispersive X-ray analysis (EDX) to investigate the mineral elemental properties of the pigments and preparation layer. The analytical voltage was set at 30kV. The accelerating voltages were 1-2mm beam diameter and the counting periods were 60-120 seconds. The minimum detectable weight concentration ranged between 0.1 and 1 weight percent.

Fourier transformed infrared spectroscopy (FT-IR)

In order to investigate pigment samples and identify the organic binder, Fourier transformed infrared (FT-IR) spectroscopy was utilized as a supplemental approach. The FT-IR spectroscopy measurements were carried out in the 400 to 4000 cm^{-1} range, with an 8 cm^{-1} spectral resolution, using an FT-IR spectrometer (Vertex 70, Bruker) fitted with an attenuated total reflection accessory.

Results and discussion

Identification of wood species

Microscopic examinations of wooden samples indicate that wood species in the body of the statue and its pedestal (Table 1) are made of two indigenous woods sycamore fig (*Ficus sycomorus* L.) (Fig. 2), Tamarisk (*Tamarix aphylla* L.) (Fig. 3) and one imported wood Lebanese Cedar (*Cedrus libani* A. Rich.) (Fig. 4); while dowels (Table 2) are made of two indigenous woods, Christ's thorn (*Ziziphus spina Christi* L. Willd) (Fig. 5), Nile tamarisk (*Tamarix nilotica* Ehrenb.) (Fig. 6) and one imported wood common box (*Buxus sempervirens* L.) (Fig. 7) [17-20].

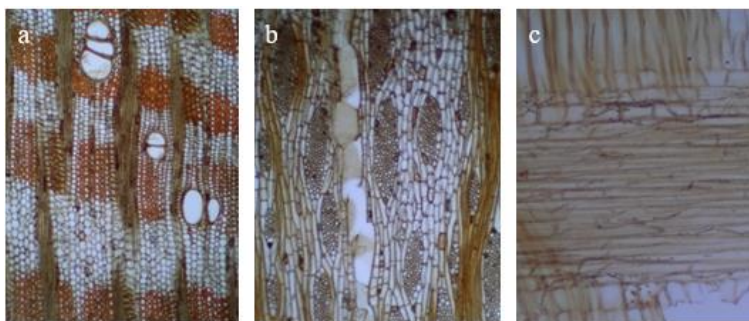


Fig. 2. Micro-images of wood slices under the microscope illustrate the anatomical properties of sycamore fig (*Ficus sycomorus* L.): a) transverse section; b) tangential longitudinal section; c) radial longitudinal section

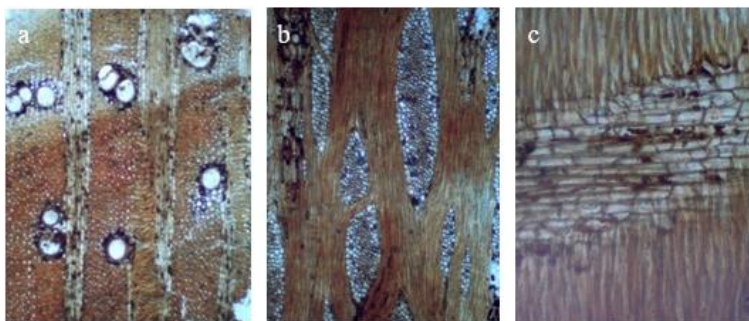


Fig. 3. Micro-images of wood slices under the microscope illustrate the anatomical properties of Tamarisk (*Tamarix aphylla* L.): a) transverse section; b) tangential longitudinal section; c) radial longitudinal section

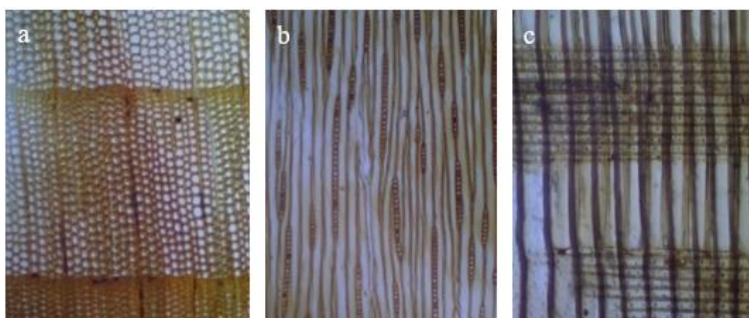


Fig. 4. Micro-images of wood slices under the microscope illustrate the anatomical properties of Lebanese Cedar (*Cedrus libani* A. Rich.): a) transverse section; b) tangential longitudinal section; c) radial longitudinal section

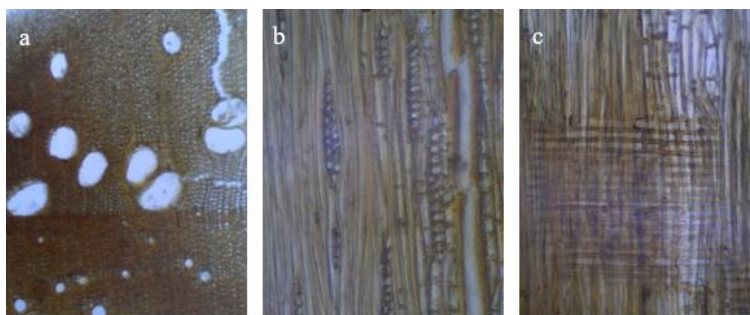


Fig. 5. Micro-images of wood slices under the microscope illustrate the anatomical properties of Christ's thorn (*Ziziphus spina christi* L.): a) transverse section; b) tangential longitudinal section; c) radial longitudinal section

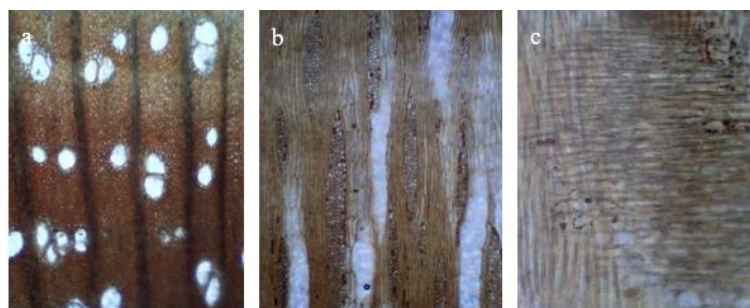


Fig. 6. Micro-images of wood slices under the microscope illustrate the anatomical properties of Nile tamarisk (*Tamarix nilotica* Ehrenb.): a) transverse section; b) tangential longitudinal section; c) radial longitudinal section.

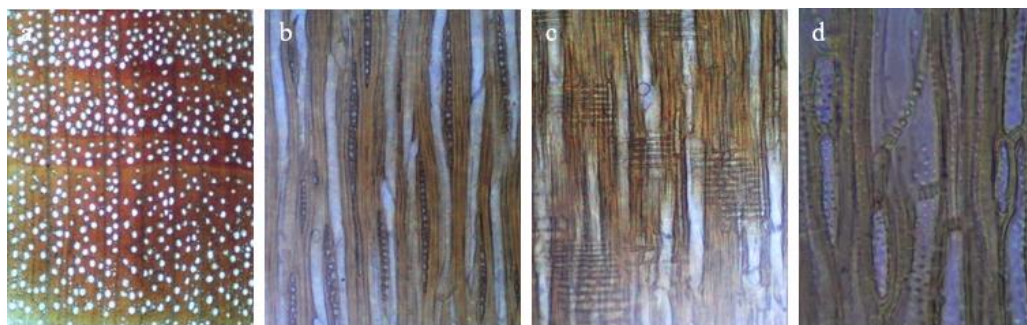


Fig. 7. Micro-images of wood slices under the microscope illustrate the anatomical properties of common box (*Buxus sempervirens* L.): a) transverse section; b) tangential longitudinal section; c) radial longitudinal section; d) Scalariform perforation plates in tangential longitudinal section

Table 1. Characteristic anatomical features of wood species in the statue body and pedestal

Anatomical characteristics	Sycamore fig <i>Ficus sycomorus</i>	Tamarisk aphylla <i>Tamarix aphylla</i>	Lebanese Cedar <i>Cedrus libani</i>
Growth rings	Absent	Faint to Distinct	Distinct
Vessel's porosity	Diffuse porous.	Diffuse to semi-ring porous.	Absent
Vessel's groupings	In multiples of 2 to 3(6), rarely solitary.	Mostly solitary, sometimes in multiples 2(4) and clusters 3-4.	---
Parenchyma arrangement	In bands (up to 20-cells wide), scanty paratracheal or vasicentric.	Vasicentric, mostly fusiform	---

Anatomical characteristics	Sycamore fig <i>Ficus sycomorus</i>	Tamarisk aphylla <i>Tamarix aphylla</i>	Lebanese Cedar <i>Cedrus libani</i>
Perforation plates	Simple	Simple	---
Ray seriation	Two distinct sizes, 1-4 seriate and 5-14 seriate.	5-23 seriate.	Rays uniseriate and in part 2-3 seriate.
Ray composition	Heterocellular composed of procumbent with 1 to 4 rows of upright and square marginal cells.	Weakly heterocellular composed of procumbent central cells and square marginal cells.	Marginal ray tracheids in single rows, and fairly thick-walled ray parenchyma cells with nodular end walls.
Crystals	Solitary, prismatic, in ordinary ray and parenchyma cells.	Solitary, prismatic in peripheral ray cells.	crystals in ray cells.
Laticifers	Observed in rays.	Absent	Absent
Sheath cells	Present	Absent	Absent

Table 2. Characteristic anatomical features of wood species used as wooden pins in *Bastet* statue.

Anatomical characteristics	Christ's thorn <i>Ziziphus spina christi</i>	Nile tamarisk <i>Tamarix nilotica</i>	common box <i>Buxus sempervirens</i>
Growth rings	Distinct	Distinct	Distinct
Vessel's porosity	Semi-ring porous to diffuse-porous.	Ring to semi ring porous.	Diffuse porous
Vessel's groupings	Vessel's solitary and in radial multiples of 2 to 4 common.	Mostly solitary, sometimes in multiples of 2(4) and clusters of 3-4.	Predominantly solitary.
Parenchyma arrangement	Axial parenchyma diffuses and scanty paratracheal.	Vasicentric; fusiform, sometimes in 2-celled strands.	Axial parenchyma diffuses and scanty paratracheal. apotracheal parenchyma in narrow bands or lines up to three cells wide.
Perforation plates	Simple	Simple	Scalariform perforation plates with less than 10 bars.
Ray seriation	Rays uniseriate to 3 cells wide.	(3) 6-12 seriate.	Ray width predominantly 1 to 3 cells. Rays with multiseriate portions as wide as uniseriate portions.
Ray composition	Rays with procumbent, square and upright cells mixed throughout the ray.	Weakly heterocellular composed of procumbent central cells and square marginal cells.	Body ray cells procumbent with 2 to more than 4 rows of square marginal cells.

Identification of isolated insects

The collected and isolated dead insects were identified as black carpet beetle (*Attagenus unicolor*) (Fig. 8a) and Spider beetles (*Gibbium psylloides*) (Fig. 8b). *A. unicolor* and *G. psylloides* are widespread in Egypt; Fur, feathers, animal skin, hair, wool, silk, yarn, carpets, bug specimens, parchment, and vellum, or stuffed creatures are among the foods they devour and have even been known to attack Egyptian mummies [21-24]. Remains of lizard skeleton (Fig. 8c) were detected inside the pedestal during the visual investigation, the authors think that this lizard trapped and dead inside the statue's hollow pedestal a long time ago.



Fig. 8. Isolated insects identified as (a) Black carpet beetle (*Attagenus unicolor*) and (b) Spider beetles (*Gibbium psylloides*) (c) Front part of a lizard's skeleton inside the pedestal

Identification of textile

Remains of textile were detected around the statue and inside the hollow pedestal; the visual and digital microscope inspection revealed several signs of insect-caused degradation, including missing and holes in the linen wrappings (Fig. 9a). Transverse dislocations, also known as cross-thatches or nodes, are used for identification along the length of the fiber; the width is usually constant throughout the length of the fiber; and the fibers have dark dislocations that are roughly perpendicular to the long axis of the fiber; depending on these characters, this textile may be linen (Fig. 9b) [25, 26]. For estimating the weaving quality, counting the threads of the warp and weft quality (Figure 9c) is 16×24 thread per 1cm^2 .



Fig. 9. Investigation of the textile: (a) Deterioration aspects of insect's attack. (b) Textile is identified as linen. (c) Textile quality 16×24 threads per 1cm^2

Stratigraphic structure

Examination of the stratigraphic structure of decorated layers by digital USB microscope show that there is a distinctive difference in decoration techniques between the gilded face of the statue, statue's body and statue's pedestal; The face composed of wooden support coated with a thin layer of textile coated with gesso layer, respectively, then a thin leaf of gold is applied over this gesso layer (Fig. 10a). The statue's body composed of wraps of textiles coated with a bright white gesso layer; while pieces of wooden support detected in the statue's body backbone, and legs (Fig. 10b).

The decoration technique in the pedestal areas consisted of wooden support coated with a white preparatory layer followed by black pigment, and then another white preparatory layer painted with several pigments coated with a waxy material in some areas (Fig. 10c).

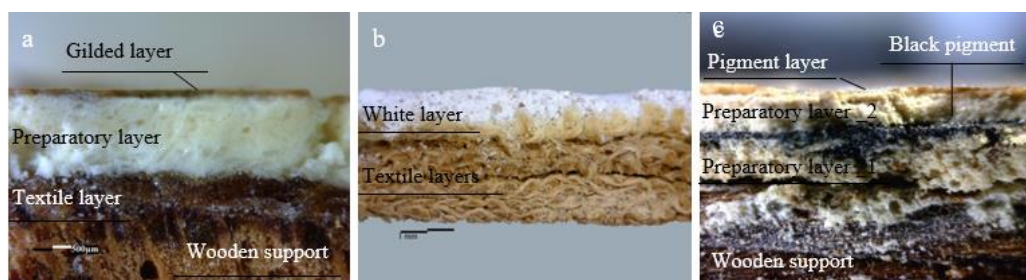


Fig. 10. Stratigraphic structure of decorated layers by digital USB microscope: (a) Gilded face (b) Body (c) Pedestal.

Technical photography

The existence of a yellowish emission from luminescent material on the pedestal surface was discovered by UV-induced luminescence (UVL) (Fig. 11b), this luminescence may be related to a natural wax used in the antiquity interventions, the ancient Egyptian used wax as a coating material. Visible-induced infrared luminescence (VIL) photography allows mapping

and detecting Egyptian blue; the Egyptian blue pigment showed up as bright white areas against a dark background (Fig. 11c). The black outlines were uncovered using infrared reflectance (IRR) photography (Fig. 11d), which were not apparent in visible light due to the dirt's negative effects.

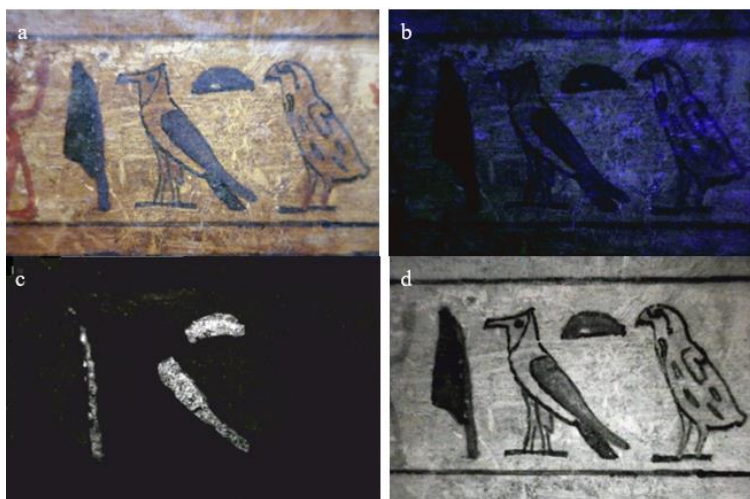


Fig. 11. Technical photography: (a) Visible light (VIS) (b) UV-induced luminescence (UVL) (c) Visible induced infrared luminescence (VIL) (d) Infrared reflected (IRR)

Raking light

The oblique light images show the strikes of antiquities brush and its directions; the bulk of the Egyptian blue is very clear on the outer surface of the pedestal, the rough surface of the blue painted layer may be seen in the photographs. Its grains were not uniformly coated or flowed off the brush, resulting in a thickness disparity from one region to the next. Furthermore, the blue pigment may have been dabbed into place for small portions rather than brushed on as is customary (Fig. 12).



Fig. 12. Strikes of brushes and Egyptian blue are clarified by oblique light

Identification of pigments and preparatory layer

White pigment

The energy dispersive X-Ray (ESEM-EDX) analysis (Fig. 13a) of white pigment on the body of the studied statue show the presence of high concentration of calcium (Ca), besides oxygen (O) and carbon (C) this result indicates that the outer white pigment may be calcium carbonate (chalk), The presence of the silicon (Si) and aluminum (Al) elements suggest possible existence of alumina-silicate and quartz (SiO_2) materials [27].

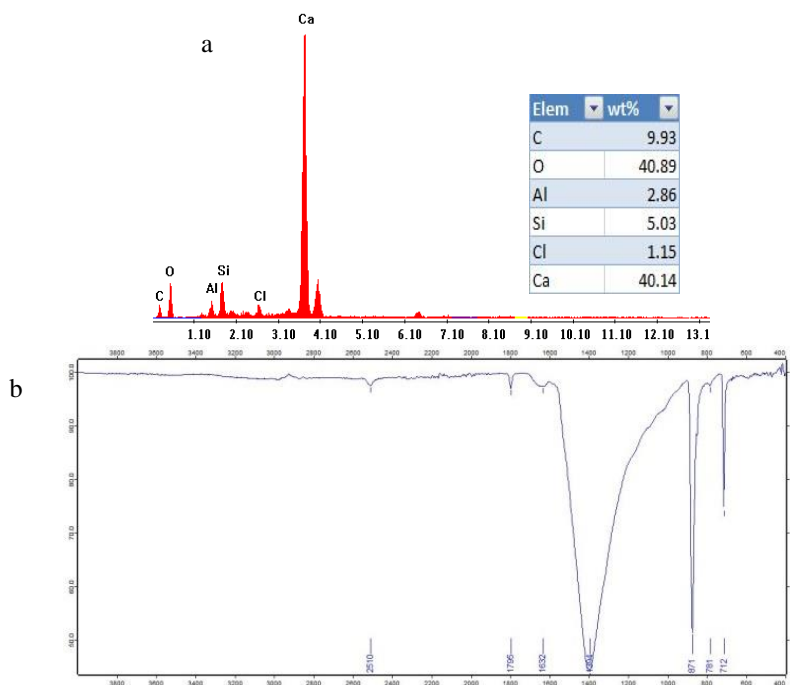


Fig. 13. Micro analysis of the White pigment (a) EDX analysis (b) FT-IR spectrum

In the (FTIR) spectrum (Fig. 13b), bands at 1394, 871 and 712cm⁻¹ are attributed to calcium carbonate due to the C–O stretching of carbonate, and the weak peaks at 1795 and 2510cm⁻¹, which are combination and overtone bands [28-29], band at 1632 cm⁻¹ probably denote the presence of calcium oxalates which are common components of degraded organic materials and band at 781cm⁻¹ attribute to quartz [30]. No clear evidence was found for an organic-based binding medium for this pigment. For a long time, the number of white hues employed in ancient Egypt was restricted to only two types of pigments: calcium carbonate (CaCO₃) derived from the mineral Calcite and calcium sulphate (as CaSO₄ or its hydrate CaSO₄·2H₂O) [31-33].

Blue pigment

Egyptian craftsmen made Egyptian blue by burning a combination of compounds comprising silicon (Si), calcium (Ca), and copper (Cu) with a soda flux during the old kingdom (2600BC) [34, 35].

According to energy dispersive X-Ray (ESEM-EDX) Silicon (Si), copper (Cu), and calcium (Ca) were the elements with the highest concentrations in the blue painted layer's spectrum (Fig.14a), this finding demonstrates the existence of a copper-based pigment, most likely Egyptian blue (CaO·CuO·4SiO₂). The data acquired by (VIL), showed the blue color appeared as bright white, the luminescence of such areas indicate the presence of Egyptian blue [36].

In the (FT-IR) spectrum of the same sample (Fig. 14b), we can detect, besides calcium carbonate (bands at 1433, 875 and 718cm⁻¹) and quartz (band at 780 cm⁻¹), Egyptian blue pigment (bands at 1325, 1162, 1004, 754 and 662 cm⁻¹) [37, 38]. The bands at ~400 and 466 cm⁻¹ indicate the presence of amorphous silicates [39].

Egyptian blue is an artificially created copper calcium silicate that has been documented in Egyptian art dating back to the 4th Dynasty. This glassy pigment, while creating a bright, durable color, requires a larger support medium than other Egyptian art colorants [40].

The (FT-IR) spectra also suggest the presence of proteinaceous and waxy binding media highlighted by the absorption band at (3307cm^{-1}) attributed to (OH) stretching due to intermolecular hydrogen bonding of the hydroxyl group and NH stretch of aliphatic primary amine, the band at (1631cm^{-1}), C = O stretching band, is assigned to amide I, while the bands at (1574 and 1545cm^{-1}) (C–N–H) is assigned to amide II indicate using proteinaceous based binding medium [11, 41]. Absorption band at 1376cm^{-1} corresponding to CH_3 symmetric deformation and band at 1462cm^{-1} corresponding to CH_2 bending, besides, an absorption carbonyl band around 1735cm^{-1} along with two sharp bands around 2915 and 2848cm^{-1} , due respectively to stretching CH_3 and CH_2 vibrations, indicated the presence of free fatty acids, absorption ascribable to natural waxes [42, 43]. The analyte signal related to the ester and free fatty acids vibration (at 1735cm^{-1}) in the infrared spectrum of blue pigment is useful and informative spectroscopic data for beeswax identification [44-46].

Beeswax, a secretion of the honeybee, is the most significant wax utilized in ancient art (*Apis mellifica*). In ancient Egypt, beeswax was utilized as a binding material as well as a varnish or coating. The oldest known use of beeswax as a binder is in mummy portraits, which are mostly from the Fayum area, several examples of beeswax being used as a binder or coating have been recognized and documented by [47-49].

Identify the protein and wax in the sample by further analysis utilizing gas chromatography mass spectrometry (GC/MS) will be helpful.

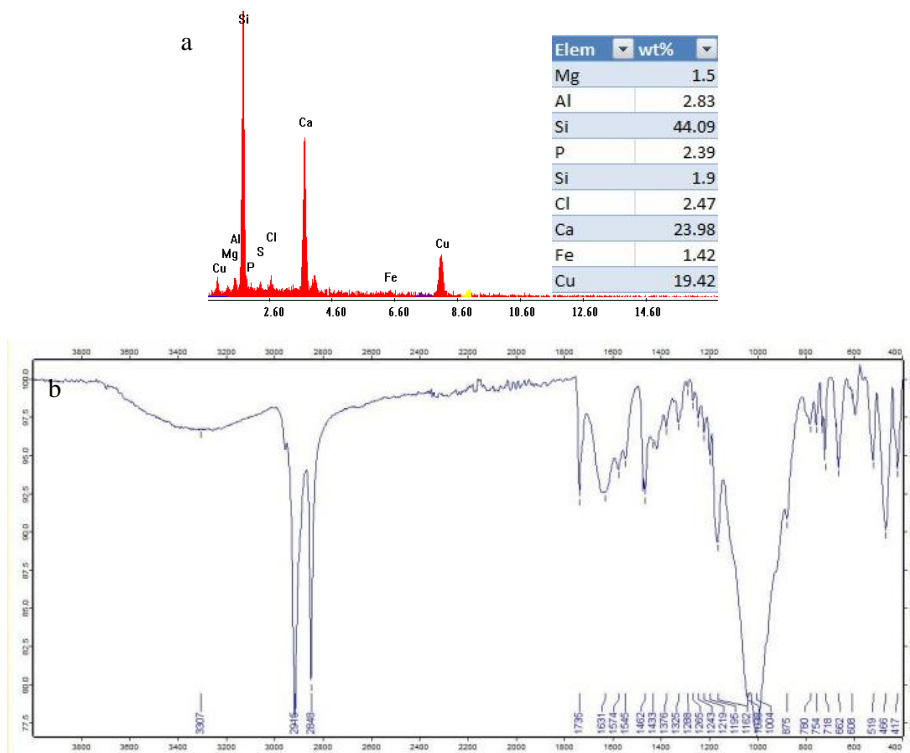


Fig. 14. Micro analysis of the blue pigment (a) EDX analysis (b) FT-IR spectrum

Red pigment

The energy dispersive X-Ray (ESEM-EDX) analysis of red pigment (Fig. 15a) showed the presence of silicon (Si), calcium (Ca), iron (Fe) and aluminum (Al) with a high intensity, in addition to a small amount of chlorine (Cl), magnesium (Mg), potassium (K), sulphur (S) and titanium (T), this result provides strong evidence for the presence of an iron-based pigment that is most likely hematite Fe_2O_3 . Natural iron oxides occur plentifully in Egypt and the majority of

red pigments used in ancient Egypt were earthen based colors containing iron oxide. Hematite ($\alpha\text{Fe}_2\text{O}_3$) was very common and has been reported by many authors [50-52]. The presence of calcium and quartz refer to the white preparatory layer.

The (FT-IR) spectrum of the red pigment (Fig. 15b) showed the presence calcium carbonate (bands in 1796 , 872 and 712cm^{-1}), quartz (band at 780cm^{-1}), silicate (band at 523cm^{-1}) and iron oxide band at (467cm^{-1}). Hematite-based pigments can show variations in the position of the hematite bands in IR spectra due to differences in particle shape and size [53-55]. The FT-IR spectra also suggest the presence of organic material, as shown by the absorption band at (3234cm^{-1}) attributed to hydroxyl group (OH), The C–H stretching vibrations occurred in the region (2915 - 2849cm^{-1}) stretching of hydrocarbons groups, the band at 1407cm^{-1} is assigned to C–H group, which by its chemical composition is similar to natural hydrocarbons such as gum Arabic. A band at 1031cm^{-1} , due to C–O, indicated the characteristics of polysaccharides, absorption bands at 1145 - 1076cm^{-1} are attributed to C–O stretching bands, the binder material may be Arabic gum [56, 57].

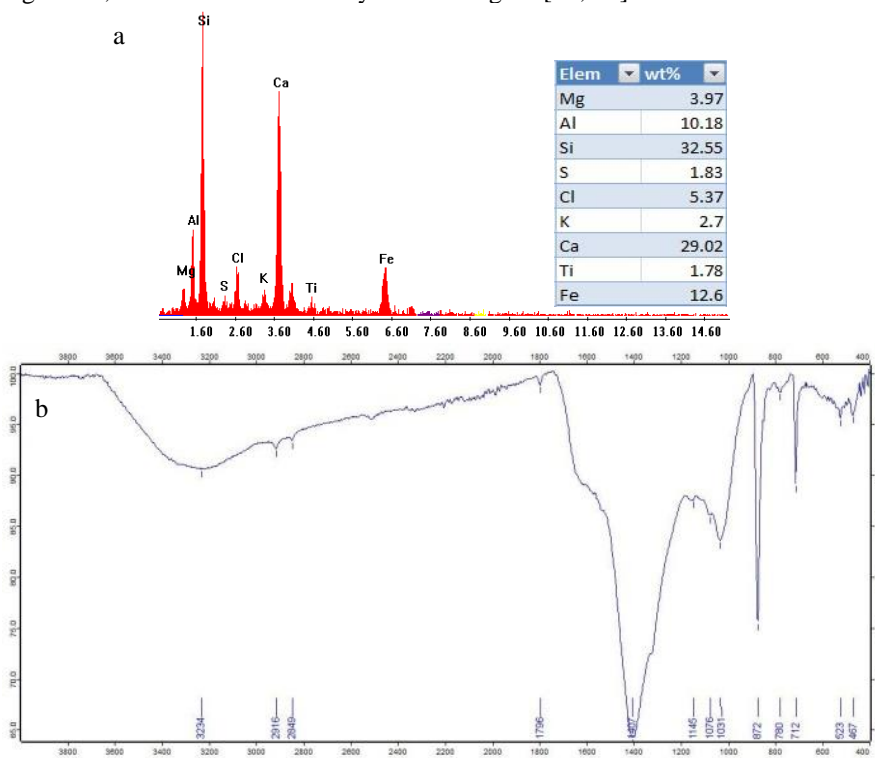


Fig. 15. Micro analysis of the red pigment (a) EDX analysis (b) FT-IR spectrum

Yellow pigment

The microanalysis data obtained by the energy dispersive X-Ray (ESEM-EDX) (Fig. 16a) proved the presence of high concentration of calcium (Ca) and silicon (Si) due to the preparatory layer which contain calcium carbonate, while the presence of sulphur (S), arsenic (As) and iron elements (Fe) suggest that the yellow pigment principally is due to using orpiment (As_2S_3) and may be mixed with small portion of goethite $\alpha\text{FeO}\cdot\text{OH}$ [53]. In earth hues like red and brown, (Al) and (K) elements are prevalent contaminants. Hematite and goethite, which are used to make ochre colors, can also be found in association with rutile (TiO_2), cuprite (Cu_2O), microcline (KAlSi_3O_8), and other minerals [58].

In (FT-IR) spectrum of the yellow pigment (Fig. 16b), bands at 3108cm^{-1} assigned to (OH) group, The C–H stretching vibrations occurred in the region (2914 - 2848cm^{-1}) stretching

of hydrocarbons groups, bands at 1796, 872 and 712cm^{-1} attribute to calcium carbonate, bands at 1397cm^{-1} are assigned to C—H group which by its chemical composition is similar to natural hydrocarbons such as gum Arabic, band at 1030cm^{-1} due to C—O, indicated the characteristics of polysaccharides. Absorption bands at $1162\text{--}1082\text{cm}^{-1}$ is attributed to C—O stretching bands, the binder material may be Arabic gum, bands at $597\text{--}523\text{cm}^{-1}$ suggests the possibility presence of orpiment (As_2S_3) and iron oxide at 464cm^{-1} [59, 60].

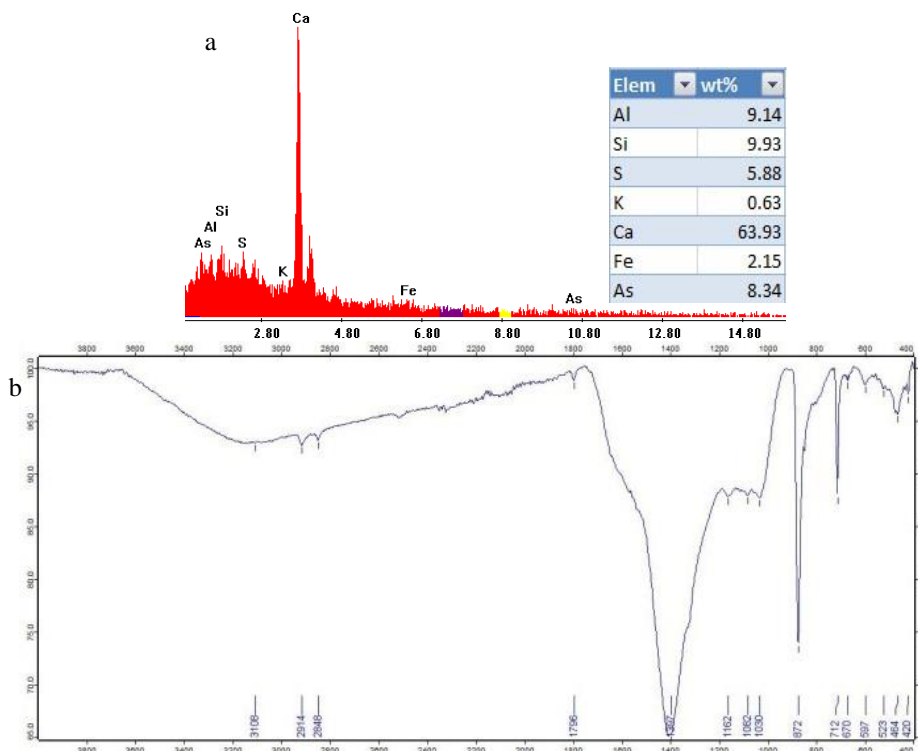


Fig. 16. Micro analysis of the yellow pigment (a) EDX analysis (b) FT-IR spectrum

Green pigment

In energy dispersive X-Ray (ESEM-EDX) analysis of the green pigment (Fig. 17a), the highest concentration elements were: (C), (O), (Si), (Ca) and (Cu); besides low portion of (Al), (Fe) and (Mg), and traces of (Cl), (P), (K) and (S). The presence of (Cu), (C) and (O) elements indicate that the green color due to copper-based pigment may be malachite $\text{CuCO}_3\text{Cu}(\text{OH})_2$ or verdigris, $\text{Cu}(\text{CH}_3\text{COO})_2 \cdot 2\text{Cu}(\text{OH})_2$, while the presence of Al, Fe, Mg and K suggest the presence of low portion of green earth, a mixture of celadonite and glauconite, $\text{K}[(\text{Al}^{\text{III}}, \text{Fe}^{\text{III}})(\text{Fe}^{\text{II}}, \text{Mg}^{\text{II}})]$, $(\text{AlSi}_3, \text{Si}_4\text{O}_{10}(\text{OH})_2)$ since the (EDX) technology can only reveal the elemental composition of the tested substances, not their chemical forms. Green earth, malachite, and verdigris were all used in ancient Egypt, according to reports. [11, 25, 58]. The presence of (Ca) and (Si) are referring to the calcium carbonate and quartz from the preparatory layer, the presence of trace of (P) indicates that may be a proteinaceous material has been used as binding medium.

The (FT-IR) spectrum of the green pigment (Fig. 17b) showed band at 3200 cm^{-1} assigned to (OH) group, the band at (1615cm^{-1}) C = O stretching band is assigned to amide I, while the band at (1538cm^{-1}) (C—N—H) is assigned to amide II indicates using proteinaceous based binding media. bands at $1395\text{--}1321\text{cm}^{-1}$ are assigned to C—H group which by its chemical composition is similar to natural hydrocarbons such as gum Arabic, absorption bands at 1163--

1040 cm^{-1} are due to C—O indicated the characteristics of polysaccharides. The authors think that the proteinaceous-based binding medium used for the preparatory layer, while Arabic gum used as binding medium for the green pigment or mixed with small amount of another protein material. The bands at 872 and 712 cm^{-1} attribute to calcium carbonate, while band at 780 cm^{-1} due to quartz [56, 57, 60].

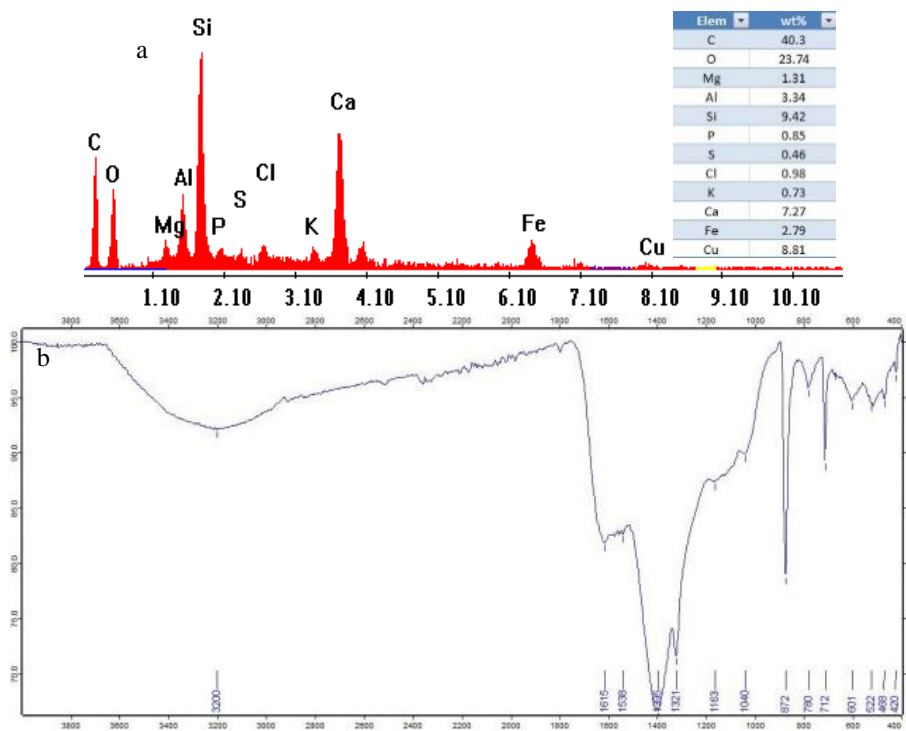


Fig. 17. Micro analysis of the green pigment (a) EDX analysis (b) FT-IR spectrum

Black pigment

In the energy dispersive X-Ray (ESEM-EDX) data of the black pigment microanalysis (Fig. 18a), (C) and (O) elements exhibit the highest concentrations. This result suggests the possibility of carbon-based black pigment; the presence of (Ca), (Si), (Al) and (Fe) may be related to calcium carbonate, quartz and clay minerals in the preparatory layer below or the black pigment is contaminated with significant amounts of other pigments such as iron oxide and green earth [62, 63]. The presence of trace of (P) indicates existence of a proteinaceous material has been used as binding medium in the preparatory layer.

The (FT-IR) spectrum of black pigment (Fig. 18b) showed the C—H stretching vibrations occurred in the region (2914–2848 cm^{-1}) stretching of hydrocarbons groups, characteristic of lipids, the band at 1642 cm^{-1} attributed to C=O stretching group, bands at 1404 cm^{-1} are assigned to C—H, C—O stretching bands at 1078–1038 cm^{-1} indicated the characteristics of polysaccharides. Calcium carbonate (absorptions in 1796, 872 and 712 cm^{-1}) and quartz (absorption at 782 cm^{-1}) can be detected [47, 63]. The particle sizes are modest, and there is no indication of a second phosphate peak about 960 cm^{-1} , which would imply the usage of a black pigment generated from bone or ivory burning. Although these pigments might have come from crushed charcoal, the small particle size and lack of evidence of cellular structure indicate that they are most likely lamp black or soot, which is created by the burning of vegetable materials or oil [42].

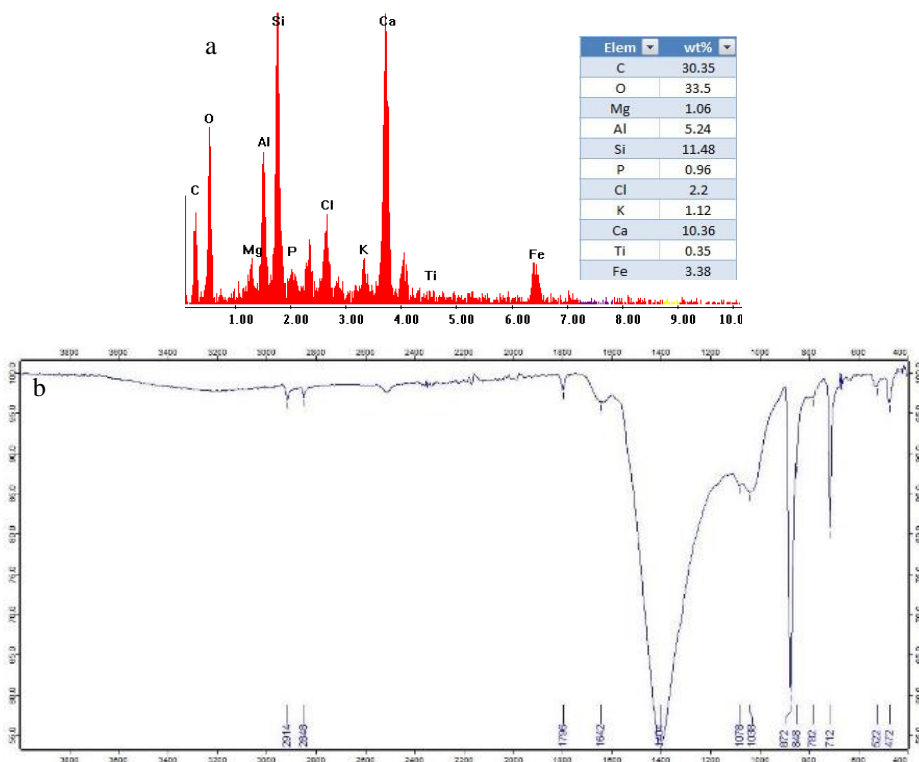


Fig. 18. Micro analysis of the black pigment (a) EDX analysis (b) FT-IR spectrum

Preparatory layer

All the energy dispersive X-Ray (ESEM-EDX) spectra, acquired on the surface of the *Bastet* statue, even on areas with no pictorial layers, showed the peaks of calcium and silicon, related to calcite (CaCO_3) and quartz (SiO_2) of the preparatory layer. (Mg), (Al) and (Cl) signals were also observed. These elements can be found as common impurities in rocks used to prepare ground layers.

The microanalysis of the preparatory layer obtained by the energy dispersive X-Ray (ESEM-EDX) (Fig. 19a) shows a high concentration of (Ca), (O), and (C) this indicate that the preparatory layer, mainly, is calcium carbonate while the presence of (Si) suggests the presence of quartz.

The (FT-IR) spectrum (Fig. 19b) indicates that the band at (3315cm^{-1}) represents (OH) hydroxyl stretching due to intermolecular hydrogen bonding of the hydroxyl group and NH stretch of aliphatic primary amine, C–H stretching vibrations occurred in the region ($2917\text{--}2849\text{cm}^{-1}$) stretching of aliphatic groups, bands at (1408 , 871 and 712cm^{-1}) are attributed to calcium carbonate and the weak peaks at 1796 and 2513cm^{-1} , which are combination and overtone bands. The band at (1622cm^{-1}) (C=O stretching band) is assigned to amide I, while the bands at ($1576\text{--}1538\text{cm}^{-1}$) (C–N–H) are assigned to amide II. Quartz can be detected by the presence of a band at (781cm^{-1}). The binder medium used with the preparatory layer is identified as proteinaceous-based medium may be animal glue [11, 64].

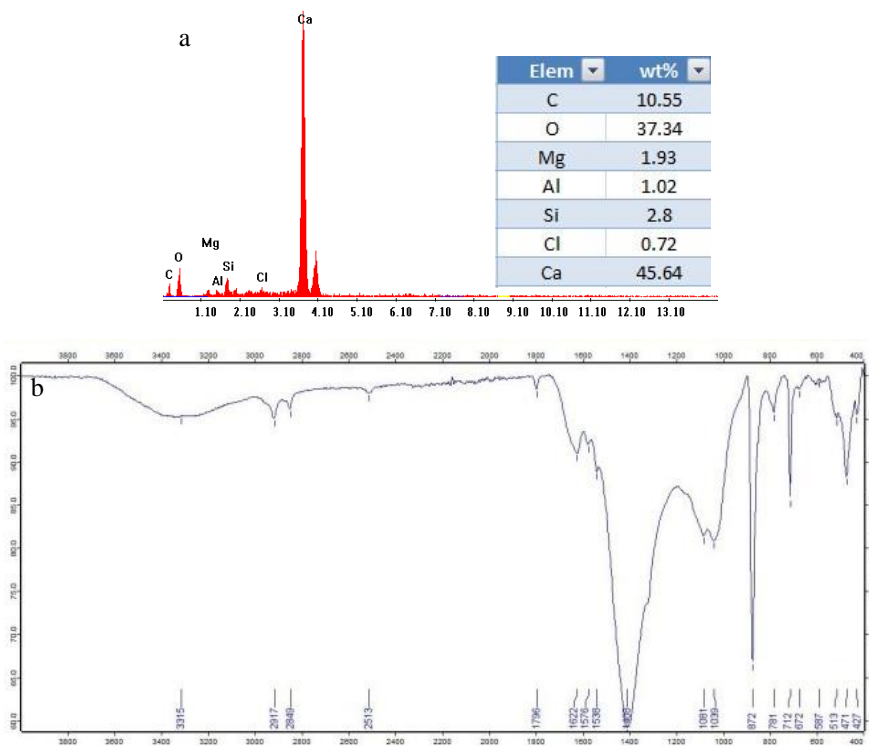


Fig. 19. Micro-analysis of the preparatory layer (a) EDX analysis (b) FT-IR spectrum

Identification of Gilded layer

Gold's unique properties, which have made it such a valuable element in business and art, were recognized by the ancient Egyptians from the beginning of history. Artefacts, or pieces of objects, created entirely of gold or decorated in part with gold, have been discovered in tombs of the first dynasty, dating back to at least 3000 B.C. [65].

The results obtained by the energy dispersive X-Ray (ESEM-EDX) analysis (Fig. 20a) indicate that analyzed gold leaf is composed of a mixture of gold (Au) 87.85% and silver (Ag) 7.15%, in additions to some impurities; according to [7, 66]. A thin sheet of pure gold or gold alloyed with minute quantities of silver, copper, or other metals was hammered into gold leaf. Traces of impurities includes (K), (Cu) and (Zn) elements can be detected, while (Ca) due to the preparatory layer.

The data obtained by (FT-IR) analysis (Fig. 20b) indicate that the sample is mainly composed of calcium carbonate (absorption bands at 871 and 712 cm^{-1}) and the weak peaks in 1796 and 2513 cm^{-1} , which are combination and overtone bands. The 1622 cm^{-1} band (O–H) may be relating to strongly held water molecules and calcium oxalate, a compound that is likely to originate from alteration processes of the original paint medium [47], the band at 1405 cm^{-1} is assigned to C–H group, which by its chemical composition is similar to natural hydrocarbons such as plant Arabic. A band at 1035 cm^{-1} due to C–O indicated the characteristics of polysaccharides; the binder material may be Arabic gum.

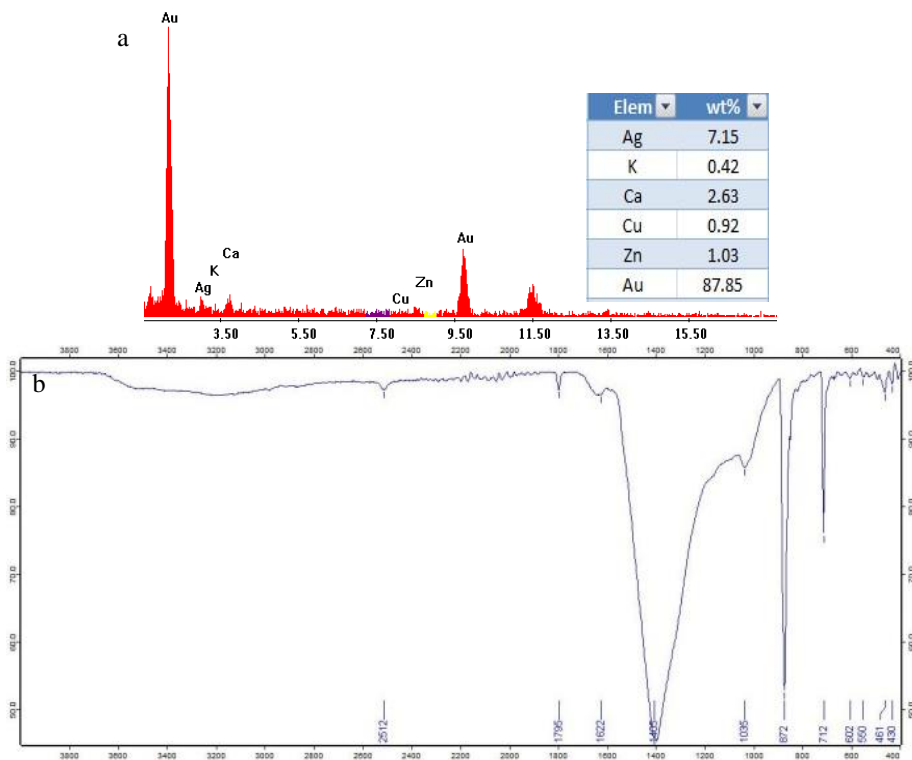


Fig. 20. Micro-analysis of the gilded layer (a) EDX analysis (b) FT-IR spectrum

Identification of waxy coating material

Visual assessment and the data acquired by visible-induced ultraviolet luminescence (UVL) (Fig. 11b) indicate the presence of organic material randomly applied over most of the painted surface of the pedestal in the antiquity interventions.

The (FT-IR) analysis (Fig. 21) showed the absorption features ascribable to a wax. bands at 2915 and 2848cm⁻¹ due to stretching C-H vibrations indicated the presence of free fatty acids and the presence of the carbonyl (C=O) stretching band at 1736cm⁻¹, that is seen in natural waxes (such as beeswax), absorption bands of C-H bending bands appear in the 1472-1463-1377cm⁻¹ and 1174-956-730-719cm⁻¹ (C-O) stretching band Their position and intensity match the spectrum profile of a natural wax, may be beeswax [28, 47].

Concerning organic materials, Due to the presence of organic coatings on the exterior surfaces, detecting and identifying binders is challenging. We identified beeswax as a covering and potentially a gum as a binder, which is consistent with similar findings in the literature [28, 47, 67-69]. The suggestion of using a proteinaceous-based medium in the preparatory layers and gum Arabic in mixture with a small amount of another protein material as a binding medium for the paint layers is supported by the results of an analysis by [47, 70].

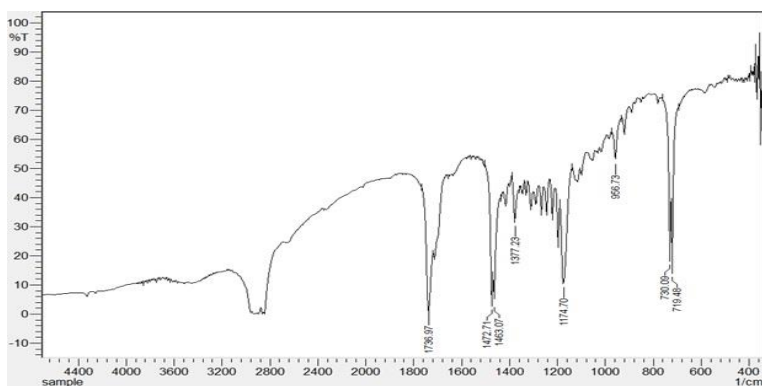


Fig. 21. FT-IR spectrum of the waxy coating material on the surface of pedestal

Conservation procedures

Condition of Bastet statue

The statue is broken into two parts the body and pedestal; in addition to, cracked, cupping, and flaking on the gilded face of *Bastet*. The polychrome pedestal is separated into small pieces of wood, closer visual examination revealed heavy damage including dirt, friable painted layers, fallen flakes, partly lifting painted layer, cracked, cupping, missing parts, and flaking polychrome on upper surfaces. There were also layers of dirt and incrustations such as mud, minerals, dust, and grimy patches inside the hollow pedestal (Fig. 22). The authors think that these aspects of deterioration are due to several factors; some of these factors include the difference in response to the changes of ambient environment (e.g. relative humidity, temperature) for the organic materials (Wooden support and textile) and inorganic materials (preparatory layer, inlaid materials), in addition to environmental of bury, environmental shock during excavation, and techniques of statue making in ancient Egypt particularly the pedestal.

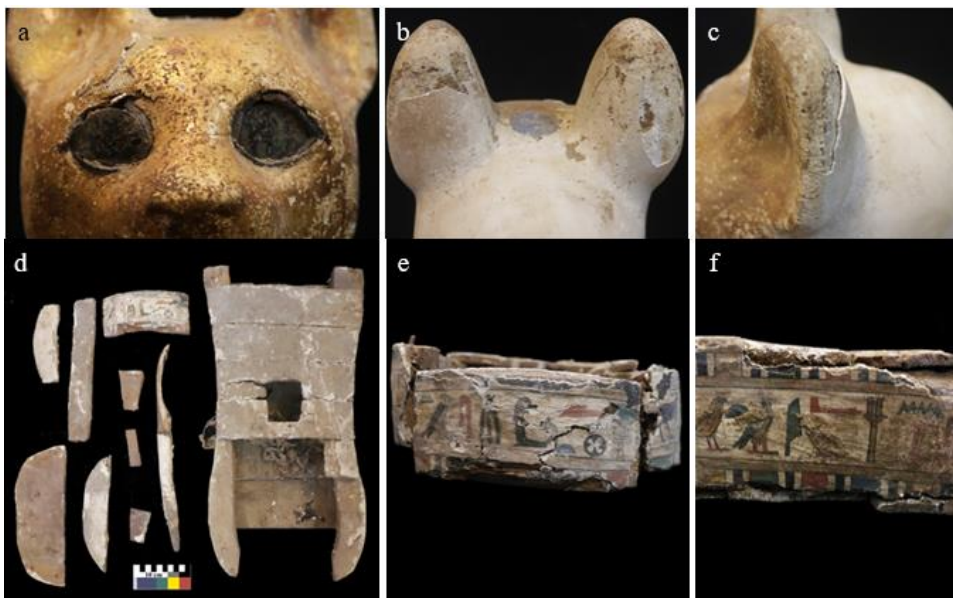


Fig. 22. Aspects of deterioration include: (a) loose and cracks of gilded layer. (b), (c) Loose, cracks and partly separation of white gesso layer. (d) Broken pedestal into many wooden pieces. (e) Deep cracks, friable and loose of painted layer. (f) Accumulations of sands and dirt

Treatment processes

Securing painted layer, Surface cleaning, and reassembling

Before any effective restoration action, the fragile gesso paint layer is protected by applying strips of Japanese paper glued with 1% w/v hydroxy propyl cellulose (Klucel G) in ethyl alcohol (Fig. 23a). After securing the paint, the restoration process included the next steps; loose dust was removed by gentle brushing. After removing grim dirt suspended using mechanical means (e.g., a scalpel and dental instruments), cotton swabs dipped in toluene and alcohol were rolled over the uneven surface to remove dirt (Fig. 23b) [1]. Wooden pieces of the pedestal were reassembled again by gluing with 60% paraloid B-72 in acetone (Fig. 23c) and clamping (Fig. 23d) [71].



Fig. 23. Conservation processes include: (a) Securing lifting flakes. (b) Cleaning and removing dirt. (c), (d) gluing, Reassembling and clamping pedestal wooden pieces

Reattaching lifted and fallen paint layers

Steps of reattaching the lifted and fallen painted layer include:

- Reinforcing the fallen flakes by back lined with strips of Japanese paper glued with 1% w/v klucel G in ethyl alcohol and left them to dry.
- A solution of 3% w/v klucel G in ethyl alcohol was used to reattaching the fallen flakes to their original place on the wooden support by brushing.
- The lifted painted layers (the face and the pedestal of the statue) were dampened on the surface with 1% methylcellulose in distilled water, and then we left it enough time before totally dried.
- To reattach lifted painted layers to wooden supports, a 3% w/v klucel G in ethyl alcohol solution was injected below the layer.
- To move the now somewhat flexible raised flakes back onto the support, treated surfaces were gently pushed with a Teflon sheet on a fingertip (Fig. 24) [2].

Fixing the statue on its pedestal

- In order to fix and reinforce the statue body on the pedestal, two cushions of balsa wood strips were fixed inside the hollow pedestal in the position of the legs and statue body (Fig. 25a & b) by 60% paraloid B-72 in acetone. For filling gaps between the statue and pedestal, cotton fibers saturated with paraloid B-72 dissolved in acetone 15% (1g/15mL) were used for filling gaps in lines of collecting points (Fig. 25c) [72].

The authors developed the ancient Egyptian technique of applying textile on the wood before applying the ground layer, the same technique has been used after substituting the natural adhesives with synthetic adhesives; textile by gauze applied on balsa wood for loss compensation; gesso layer by a mixture of 15% w/v paraloid B-72 in acetone, glass micro balloons, and earthen oxides; was applied over the gauze until the outer surface reached the expected level (Fig. 25d, e and f). After preservation, the statue is ready for storing or exhibition (Fig. 26).



Fig. 24. Reattaching fallen flakes: (a) & (b) Lining (c) Reattaching



Fig. 25. Fixing statue on its pedestal include: (a), (b) cushions of balsa wood strips. (c) Filling gaps. (d), (e) and (f) shaping balsa wood and developing ancient Egyptian techniques for missing part



Fig. 26. Bastet's statue after conservation

Conclusions

This study gives an account of the archaeometric and manufacturing techniques found in the goddess *Bastet* polychrome statue dates back to (late period, 664-332 BC), discovered in Saqqara necropolis by the Egyptian mission headed by the general secretary of (SCA). The combination of optical microscopy, technical photography (TP), and spectroscopy techniques (EDX and FT-IR), along with the visual inspection of the artwork, indicates that unusual and distinguish techniques have been used in manufacturing this statue.

The results showed that the wood used on the statue is not limited to one or two species, but instead, six species of wood. Sycamore fig (*Ficus sycomorus* L.), Tamarisk (*Tamarix aphylla* L.) and the Lebanese Cedar (*Cedrus libani* A.Rich.) were used in manufacturing the body and pedestal, while dowels were made of Christ's thorn (*Ziziphus spina christi* L.Willd), Nile tamarisk (*Tamarix nilotica* Ehrenb.) and common box (*Buxus sempervirens* L.).

Stratigraphy structure of the studied statue showed several and rare techniques of statuary-making; These results reveal that the Egyptian artisans used wraps of textile as a main component for the body and wooden pieces at the statue's backbone and legs to impose it the enough strength to fix on the pedestal, while for making the pedestal, slightly complex, small pieces of wood, whatever the most readily available in the workshop, irrespective of its particular properties, were collected together by wooden dowels, and then coated with a decoration layer made of a white preparatory layer followed by black pigment, and then another white preparatory layer painted with several pigments and coated with waxy material in some areas.

Spectroscopy techniques (EDX-FTIR) and (TP) images obtained by Dino-Lite USB digital microscope provide valuable information about the pigments, organic media and coating material. UV-induced luminescence revealed the presence of a yellowish emission from luminescent natural wax on the pedestal surface used in the antiquity interventions. Visible-induced infrared luminescence (VIL) photography allows mapping and detecting Egyptian blue, Egyptian blue pigment shows up as bright white areas against a dark background. Infrared reflected photography (IRR) revealed the black outlines, which did not clearly appear in the visible light due to the negative impacts of the dirt. The chromatic palette used in the statue identified as calcium carbonate (chalk) for white, Egyptian blue for blue, hematite for red, orpiment and may be mixed with small portion of goethite for yellow, malachite with low portion of green earth for green and carbon from lamp black or soot origin for black. The (EDX) results proved that the gilded layer is composed of a mixture of gold and silver.

For the organic materials (binders and coating), Due to the presence of organic coatings on the exterior surfaces, detecting and identifying binders is challenging. We could recognize beeswax as a coating layer and plant gum as a binder for the pigments of red, yellow and black, while possibly plant gum mixed with small amount of another protein material for the green pigment. Proteinaceous-based binding medium possibly animal glue used for the Egyptian blue due to its grains relatively large size and also with the preparatory layer.

Acknowledgments

The authors are very grateful to Dr. Moustafa Waziri secretary general of the Supreme Council of Antiquities and head of Egyptian mission in Saqqara site, for continuous supporting. We also thank the members of the Egyptian mission and administration of conservation in Saqqara for the valuable information. We would also like to thank conservators of museum storerooms conservation and administration of storeroom No. 2 for all their insightful comments and suggestions.

References

- [1] M. Abdallah, H.M. Kamal, A. Abdrabou, *Investigation, preservation and restoration processes of an ancient Egyptian wooden offering table*, **International Journal of Conservation Science**, **7**(4), 2016, pp.1047-1064.
- [2] M. Abdallah, A. Abdrabou, H.M. Kamal, *Analytical study and conservation processes of Tutankhamen decorated stick: a case study*, **Scientific Culture**, **4**(1), 2018, pp. 93-100.
- [3] L.A. Donaldson, *Analysis of fibers using microscopy: Fundamentals and manufactured polymer fibres*, **Handbook of Textile Fibre Structure**, (Editors: S.J. Eichhorn, J.W.S. Hearle, M. Jaffe and T. Kikutani), Woodhead Publishing Limited, 2009, pp. 121-153.
- [4] J.K. Delaney, E. Walmsley, B. H. Berrie, C. F. Fletcher, *Multi-spectral imaging of paintings in the infrared to detect and map blue pigments*, **Scientific Examination of Art Modern Techniques in Conservation and Analysis**, National Academies Press, Washington, 2005, pp.120-136.
- [5] A. Abdrabou, M. Abdallah, H.M. Kamal, *Scientific investigation by technical photography, OM, ESEM, XRF, XRD and FTIR of an ancient Egyptian polychrome wooden coffin*, **ConservarPatrimónio**, **26**, 2017, pp. 51-63.
- [6] A. Abdrabou, M. Abdallah, I. Shaheen, H.M. Kamal, *The application of multispectral imaging and reflectance transformation imaging to an ancient Egyptian polychrome wooden stela*, **The 18th Triennial Conference of the International Council of Museums Committee for Conservation (ICOM.CC)**, Copenhagen, Denmark, 2017.
- [7] A. Cosentino, *Practical notes on ultraviolet technical photography for art examination*, **ConservarPatrimónio**, **21**, 2015, pp.53-62.
- [8] G. Verri, M. Gleba, J. Swaddling, T. Long, J. Ambers, T. Munden, *Etruscan women's clothing and its decoration: the polychrome gypsum statue from the 'Isis Tomb' at Vulci*, **The British Museum Technical Research Bulletin**, **8**, 2014, pp. 59-71.
- [9] G. Verri, C. Clementi, D. Comelli, S. Cather, F. Pique, *Correction of Ultraviolet-Induced Fluorescence Spectra for the Examination of Polychromy*, **Applied Spectroscopy**, **62**(12), 2008, pp.1295-1302.
- [10] B. Stuart, **Analytical Techniques in Materials Conservation**, John Wiley & Sons Ltd, Chichester, 2007.
- [11] A. Abdrabou, M. Abdallah, I. Shaheen, , H.M. Kamal, *Investigation of an ancient Egyptian polychrome wooden statuette by imaging and spectroscopy*, **International Journal of Conservation Science**, **9**(1), 2018, pp. 39-54.
- [12] E. Passmore, J. Ambers, C. Higgitt, C. Ward, B. Wills, S. Simpson, C. Cartwright, *Hidden, looted, saved: the scientific research and conservation of a group of Begram Ivories from the National Museum of Afghanistan*, **The British Museum Technical Research Bulletin**, **6**, 2012, pp. 33-46.
- [13] G. Verri, D. Saunders, J. Ambers, T. Sweek, *Digital mapping of Egyptian blue: Conservation implications*, **Studies in Conservation**, **55**(Sup 2), 2010, pp. 220-224, <http://dx.doi.org/10.1179/sic.2010.55.Supplement-2.220>.
- [14] J. Dyer, G. Verri, J. Cupitt, **Multispectral Imaging in Reflectance and Photo-induced Luminescence Modes: A User Manual**, The British Museum, London, 2013.
- [15] A. Cosentino, *Identification of pigments by multispectral imaging; A flowchart method*, **Heritage Science**, **2**, 2014, Article number: 8.
- [16] M. Abdallah, A. Abdrabou, H.M. Kamal, *Multisientific analytical approach of polychrome Greco-Roman palette applied on a wooden model naos: case study'*, **Mediterranean Archaeology and Archaeometry Journal**, **20**(2), 2020, pp. 45-65.
- [17] * * *, IAWA Committee, *List of microscopic features for softwood identification*, **IAWA Journal**, **25**, 2004, pp. 1-70.
- [18] A. Crivellaro, F.H. Schweingruber, **Atlas of Wood, Bark and Pith Anatomy of Eastern Mediterranean Trees and Shrubs with Special Focus on Cyprus**, Springer-Verlag, Berlin, 2013.

- [19] * * *, *Tamarix aphylla*, in the inside wood database, <https://insidewood.lib.ncsu.edu/description?5> [accessed 2020-11-16].
- [20] * * *, *Tamarix nilotica*, in the inside wood database, <https://insidewood.lib.ncsu.edu/results?3> [accessed 16-11-2021].
- [21] * * *, <https://museumpests.net/wp-content/uploads/2019/03/Black-Carpet-Beetle-1.pdf> [accessed 12-09-2021].
- [22] N. David, **Identifying Insect Pests in Museums and Heritage Buildings**, The Natural History Museum, 2018.
- [23] * * *, National Park Service, *Identifying Museum Insect Pest Damage*, **Conserve o Gram**, 3(11), 2008, pp. 1-7.
- [24] **Identification of Museum Pests**, <http://museumpests.net/identification/> [accessed 15-12-2020].
- [25] M.E. Florian, *Identification of Plant and Animal Materials in Artefacts*, **The Conservation of Artifacts Made from Plant Materials** (Editors: M.E. Florian, D.P. Kronkright and R.E. Norton), The Getty Conservation Institute, 1990.
- [26] * * *, The Identification of Natural Fibres - Canadian Conservation Institute (CCI) Notes 13_18 – Canada, <https://www.canada.ca/en/conservation-institute/services/conservation-preservation-publications/canadian-conservation-institute-notes/identification-natural-fibres.html> [accessed 17-12-2020].
- [27] H. Mahmoud, *A preliminary investigation of ancient pigments from the mortuary temple of Seti I, el-Qurna (Luxor, Egypt)*, **Mediterranean Archaeology and Archaeometry**, 11(1), 2011, pp. 99-106.
- [28] S. Bracci, O. Caruso, M. Galeotti, R. Iannaccone, D. Magrini, D. Picchi, D. Pinna, S. Porcinai, *Multidisciplinary approach for the study of an Egyptian coffin (late 22nd/ early 25th dynasty): Combining imaging and spectroscopic techniques*, **Spectrochimica Acta Part A: Molecular and Biomolecular Spectroscopy**, 145, 2015, pp. 511-522.
- [29] E. L. Kendix, *Transmission and Reflection (ATR) Far-Infrared Spectroscopy Applied*, **The Analysis of Cultural Heritage Materials**, Università di Bologna, 2009.
- [30] F. Bosch Reig, J.V. Gimeno Adelantado, M.C. Moya Moreno, *FTIR quantitative analysis of calcium carbonate (calcite) and silica (quartz) mixtures using the constant ratio method, Application to geological samples*, **Talanta**, 58, 2002, pp. 811-821.
- [31] A. Heywood, *The use of huntite as a white pigment in ancient Egypt*, **Colour and Painting in Ancient Egypt**, (Editor: W.V. Davies), Oxbow Books, London, 2001, pp. 5-9.
- [32] A. Lucas, J. Harris, **Ancient Egyptian Materials and Industries**, Histories and Mysterious of man, London, 1989, pp. 348-349.
- [33] L. Lee, S. Quirke, *Painting materials*, **Ancient Egyptian Materials and Technology**, (Editors: I. Shaw and P. Nicholson), The American University in Cairo Press, Cambridge, L, 2000, pp. 104-119.
- [34] S. Pagès-Camagna, S. Colinart, *The Egyptian green pigment: its manufacturing process and links to Egyptian blue*, **Archaeometry**, 45(4), 2003, pp. 637-658.
- [35] S. Pages-Camagna, H. Guichard, *Egyptian colours and pigments in French collections: 30 years of physicochemical analyses on 30 objects*, **Decorated Surfaces on Ancient Egyptian Objects Technology, Deterioration and Conservation**, (Editors: J. Dawson, C. Rozeik and M.M. Wright), **Proceedings of a Conference Held in Cambridge, UK, in Association with the Fitzwilliam Museum, Cambridge Research Institute of Conservation**, Archetype Publications, London (2010)25-31.
- [36] G.A. Mazzocchin, F. Agnoli, M. Salvadori, *Analysis of Roman age wall paintings found in Pordenone, Trieste and Montegrotto*, **Talanta**, 64, 2004, pp. 732-41.
- [37] L. Lluveras, A. Torrents, P. Giráldez, M. Vendrell-Saz, *Evidence for the use of Egyptian blue in an 11th century mural altarpiece by SEM-EDS, FTIR AND SR XRD (church of santpere, Terrassa, Spain)*, **Archaeometry**, 52(2), 2010, pp. 308-319.

- [38] A. Shoeib, *Examination of pigments and organic binding media applied on ancient Egyptian wall paintings dating from the New Kingdom (1348–1320BC)*, **Zabytkoznawstwo konserwatorstwo**, **30**, 1998, pp. 132-142.
- [39] H. Mahmoud, *A Multianalytical approach for characterizing pigments from the tomb of Djehutyemhab (TT194), EL-Qurna necropolis, Upper Egypt*, **Archeometriai Műhely**, **3**, 2012, pp. 205-214.
- [40] J. Ambers, *Raman analysis of pigments from the Egyptian Old Kingdom*, **Journal of Raman Spectroscopy**, **35**, 2004, pp. 768-773.
- [41] H. Afifi, *Analytical investigation of pigments, ground layer and media of cartonnage fragments from Greek Roman period*, **Mediterranean Archaeology and Archaeometry Journal**, **11**(2), 2011, pp. 91-98.
- [42] L. Bonizzoni, S. Bruni, V. Guglielmi, M. Milazzo, O. Neri, *Field and laboratory multi-technique analysis of pigments and organic painting media from an Egyptian coffin (26th dynasty)*, **Archaeometry**, **53**(6), 2011, pp. 1212-1230.
- [43] V. Vyshniak, O. Dimitriev, S. Litvynchuk, V. Dombrovskiy, *Identification of beeswax and its falsification by the method of infrared spectroscopy*, **Ukrainian Food Journal**, **7**(3), 2018, pp. 421-433.
- [44] L. Svečnjak, G. Baranović, M. Vinceković, S. Prđun, D. Bubalo, I. Gajger, *An Approach for routine analytical detection of beeswax adulteration using FTIR-ATR spectroscopy*, **Journal of Apicultural Science**, **59**(2), 2015, pp. 37-49.
- [45] I.C.A. Sandu, C. Luca, I. Sandu, M. Pohontu, *Research regarding the soft wood support degradation evaluation in old paintings, using preparation layers. II. IR and FTIR Spectroscopy*, **Revista de Chimie**, **52**(7-8), 2001, pp.409-419.
- [46] A. Ghavidel, I. Sandu, V. Vasilache, *Decay Resistance of Beech Wood Against White Rot Fungus*, **Acta Chemica Iasi**, **28**(2), 2020, pp.175-182. DOI10.2478/achi-2020-0012.
- [47] C. Brøns, K. Rasmussen, M. Crescenzo, R. Stacey, T. Lluveras, *Painting the Palace of Apries I: ancient binding media and coatings of the reliefs from the Palace of Apries, Lower Egypt*, **Heritage science**, **6**, 2018, Article number: 6.
- [48] A. Agoranou, A. Kalliga, U. Kanakari, V. Pashalis, *Pigment analysis and documentation of two funerary portraits, which belong to the collection of the Benaki Museum*, **Portraits and masks: burial customs in Roman Egypt** (Editor: M. Bierbrier), British Museum Press, 91, London, 1997.
- [49] L. Spaabæk, *Conservation of mummy portraits at the Ny Carlsberg Glyptotek*, **Living images, Egyptian funerary portraits in the Petrie Museum** (Editor: J. Picton), Walnut Creek, 2007, p. 123.
- [50] C. Calza, R. Freitas, A. Brancaglion, R. Lopes, *Analysis of artefacts from Ancient Egypt using an EDXRF portable system*, **International Nuclear Atlantic Conference – INAC**, 2011, pp. 24-28.
- [51] K. Huhnerfuß, A. Von Bohlen, D. Kurth, *Characterization of pigments and colors used in ancient Egyptian boat models*, **Spectrochimica Acta, Part B**, **61**, 2006, pp. 1224-1228.
- [52] M. Uda, S. Sassa, S. Yoshimura, J. Kondo, M. Nakamura, Y. Ban, H. Adachi, *Yellow, red and blue pigments from ancient Egyptian palace painted walls*, **Nuclear Instruments and Methods in Physics Research, B**, **161-163**, 2000, pp.758-761.
- [53] J. Dyer, E. O’Connell, A. Simpson, *Polychromy in Roman Egypt: A study of a limestone sculpture of the Egyptian god Horus*, **Technical Research Bulletin, The British Museum**, **8**, 2014, pp. 93-103.
- [54] H. Mahmoud, L. Papadopoulou, *Archaeometric Analysis of Pigments from the Tomb of Nakht-Djehuty (TT189), El-Qurna Necropolis, Upper Egypt*, **ArcheoSciences**, **37**, 2013, pp. 19-32.
- [55] S. Vahura, U. Knuutinen, I. Leitoa, *ATR-FT-IR spectroscopy in the region of 500–230cm⁻¹ for identification of inorganic red pigments*, **Spectrochimica Acta Molecular and Biomolecular Spectroscopy, Part A**, **73**, 2009, pp. 764-771.

- [56] (ATR-FTIR spectrum of gum Arabic) <https://spectra.cs.ut.ee/paint/binders/gum-arabicum/> (accessed 25-12-2020).
- [57] R. Derrik, D. Stulik, M. Landy, **Scientific Tools for Conservation: Infrared Spectroscopy in Conservation Science**, The Getty Conservation Institute, Los Angeles, 1999.
- [58] C. Calza, M.J. Anjos, S.M.F.M. De souza, A. Brancaglion, R. Lopes, *X-ray microfluorescence with synchrotron radiation applied in the analysis of pigments from ancient Egypt*, **Applied Physics, A**, **90**, 2008, pp. 75-79.
- [59] * * *, **ATR-FTIR Spectrum of Orpiment**, https://spectra.cs.ut.ee/oil_color/orpiment-linseed-oil/ [accessed 29-12-2020].
- [60] G. Abdel-Maksoud, *Analytical techniques used for the evaluation of a 19th century quranic manuscript conditions*, **Measurement**, **44**, 2011, pp. 1606-1617.
- [61] G. Mazzochin, F. Agnoli, S. Mazzochin, I. Colpo, *Analysis of pigments from Roman wall paintings found in Vicenza*, **Talanta**, **61**, 2003, pp. 565-572.
- [62] M. Berry, *A study of pigments from a Roman Egyptian shrine*, **AICCM Bulletin**, **24**, 1999, pp.1-9.
- [63] E. Tomasini, B. Gómez, E. Halac, M. Reinoso, E. Liscia, G. Siracusano, M. Maier, *Identification of carbon-based black pigments in four South American polychrome wooden sculptures by Raman microscopy*, **Heritage Science**, **3**(19), 2015.
- [64] R. Mazzeo, S. Prati, M. Quaranta, E. Joseph, E. Kendix, M. Galeotti, *Attenuated total reflection micro FTIR characterization of pigment–binder interaction in reconstructed paint films*, **Analytical and Bioanalytical Chemistry**, **392**, 2008, pp. 65-76.
- [65] T.G. James, *Gold Technology in Ancient Egypt, mastery of metal working methods*, **Gold Bulletin**, **2**(5), 1972, pp. 35-42.
- [66] P. Hatchfield, R. Newman, *Ancient Egyptian gilding methods*, **Gilded Wood Conservation and History**, (Editors: D. Bigelow, E. Cornu, G. Landrey and C. van Home), Sound View Press, Madison CT, 1991, pp. 291-299.
- [67] G. Chiavari, D. Fabbri, G. Galletti, R. Mazzeo, *Use of analytical pyrolysis to characterize Egyptian painting layers*, **Cromatographia**, **40**, 1995, pp. 594-600.
- [68] R. Newman, M. Serpico, *Adhesives and binders*, **Ancient Egyptian Materials and Technology**, (Editors: I. Shaw and P. Nicholson), The American University in Cairo Press, Cambridge.L, 2000, pp. 475-492.
- [69] S. Bonizzoni, V. Bruni, M. Guglielmi, M. Milazzo, O. Neri, *Field and laboratory multi-technique analysis of pigments and organic painting media from an Egyptian coffin (26th dynasty)*, **Archaeometry**, **53**(6), 2011, pp. 1212-1230.
- [70] D. Scott, S. Warmlander, J. Mazurek, S. Quirke, *Examination of some pigments, grounds and media from Egyptian cartonnage fragments in the Petrie Museum, University College London*, **Journal of Archaeological Science**, **36**(3), 2009, pp. 923-932.
- [71] M. Moustafa, M. Abdallah, R. Magdy, A. Abdrabou, I. Shaheen, H. M. Kamal, *Analytical study and conservation processes of scribe box from old kingdom*, **Scientific Culture**, **3**(3), 2017, pp. 13-24.
- [72] A. Abdrabou, M. Abdallah, M. Abd Elkader, *Analytical study and conservation processes of a painted wooden Greco-Roman coffin*, **International Journal of Conservation Science**, **6**(4), 2015, pp. 573-586.

Received: June 02, 2021

Accepted: April 24, 2022